

# Quantum Chemical Methods for the Investigation of Photoinitiated Processes in Biological Systems: Theory and Applications

Andreas Dreuw<sup>\*[a]</sup>

*With the advent of modern computers and advances in the development of efficient quantum chemical computer codes, the meaningful computation of large molecular systems at a quantum mechanical level became feasible. Recent experimental effort to understand photoinitiated processes in biological systems, for instance photosynthesis or vision, at a molecular level also triggered theoretical investigations in this field. In this Minireview, standard quantum chemical methods are presented that are applicable and recently used for the calculation of excited states of photoinitiated processes in biological molecular systems. These*

*methods comprise configuration interaction singles, the complete active space self-consistent field method, and time-dependent density functional theory and its variants. Semiempirical approaches are also covered. Their basic theoretical concepts and mathematical equations are briefly outlined, and their properties and limitations are discussed. Recent successful applications of the methods to photoinitiated processes in biological systems are described and theoretical tools for the analysis of excited states are presented.*

## 1. Introduction

Photoinitiated processes play important roles in many living organisms. Plants, algae, and bacteria absorb sunlight to perform photosynthesis<sup>[1,2]</sup> and convert water and carbon dioxide into oxygen and carbohydrates, thus forming the basis for life on Earth. The vision of animals and humans is accomplished in the eye by a protein called rhodopsin, which upon absorption of a photon performs an ultrafast isomerization of the central retinal chromophore.<sup>[3,4]</sup> Many other biological functions, for instance phototaxis of bacteria and plants<sup>[4]</sup> or sensing of the Earth's magnetic field by birds,<sup>[5]</sup> start with photoexcitation of a pigment protein followed by complicated processes comprising, for example, electron transfer, excitation energy transfer, isomerization, or other reactions.

With the advent of ultrafast spectroscopy, it is now possible to study the evolution of molecular reactions experimentally on a sub-picosecond timescale, sometimes with a resolution of only a few tens of femtoseconds. In recent years, techniques such as transient absorption spectroscopy or fluorescence up-conversion have been applied to biological systems to study photoinitiated processes like those mentioned above. Very often, the resulting spectra are complicated and difficult to interpret, and theoretical assistance is needed. Also within the last 10 years, computer technology has advanced substantially making the calculation of ever larger molecules feasible. Still, by employing highly accurate methods one reaches the computational limit for molecular size quite quickly. At present, molecules with approximately 20 atoms of the second row of

the periodic table can be calculated with "chemical accuracy"<sup>1</sup> on a typical computer cluster within about a week of computation time.

As a consequence, if one wishes to study photoinitiated processes in biological systems theoretically, one immediately faces a dilemma. On the one hand, light-induced processes always demand a quantum treatment of the electronic structure, since absorption and fluorescence as well as the subsequent, usually ultrafast, photochemical processes are quantum mechanical events. On the other hand, biological systems are usually large molecular assemblies comprising several hundreds, sometimes thousands, of atoms making a quantum mechanical treatment of all electrons and nuclei impossible. To overcome this dilemma, one is forced to resort to molecular and theoretical models that capture the physical properties of the pigment protein of interest. Indeed, the absorption of a photon and the subsequent ultrafast processes, which are faster than a few hundred picoseconds, usually occur in a small spatial region of the protein and are mostly governed by only a few nuclear degrees of freedom of the pigment. The remaining protein environment has often only negligible influence on the relevant excited states of the pigment compared to the errors of the applied, necessarily approximate, theory. This makes the construction of small molecular models possible and allows for the employment of electronic structure the-

[a] Dr. A. Dreuw  
Institut für Physikalische und Theoretische Chemie  
Johann Wolfgang Goethe-Universität  
Max von Laue-Str. 7, 60438 Frankfurt am Main (Germany)  
Fax: (+49) 69-798-29709  
E-mail: andreas.dreuw@theochem.uni-frankfurt.de

<sup>1</sup> Chemical accuracy refers to the typical accuracy of a chemical experiment of about 1 kcal mol<sup>-1</sup> for relative energies and reaction barriers and less than 1% error for geometrical parameters.

ories to study the initial reactions with gradient techniques, without bothering about many nuclear degrees of freedom or slow protein motions. However, if one wants to study the effects of photoinitiated processes on longer timescales of nanoseconds and more, one must investigate the protein environment, since the initial excitation of the pigment induces large-scale structural changes of the protein, which finally lead to signal transduction. This can be accomplished by treating the protein that is not included in the quantum mechanical region classically, thus neglecting all quantum effects. In general, this strategy is summarized under the notion of quantum mechanical/molecular mechanical (QM/MM) approaches.<sup>[6,7]</sup>

The typical size of a molecular model for a pigment protein that needs to be described quantum mechanically ranges from 20 up to 200 atoms depending on the pigment molecule and the influence of the surrounding protein. For example, in blue light receptors such as photoactive yellow protein the light-absorbing pigments are usually small, and thus a molecular QM model of approximately 30 atoms can be sufficient. On the contrary, in light-harvesting complexes the pigments are huge, and QM models of more than 200 atoms can be demanded to study pigment–pigment interactions. Clearly, such models are still too large to be tractable with highly accurate quantum chemical methods, and thus one is restricted to more approximate and less accurate methods, which are computationally less expensive. For electronic ground states, density functional theory (DFT)<sup>[8–10]</sup> constitutes a reliable black-box method and, most importantly, it represents an ideal compromise between accuracy and computation time. It has thus become the workhorse for the calculation of ground-state properties of medium-sized to large molecules in all areas of chemistry, physics, and biology. Due to its good performance, DFT is successfully applied within QM/MM schemes. Unfortunately, as we will see later, no comparably reliable and computationally cheap method exists for the quantum chemical calculation of the excited states that determine photoinitiated processes.

Before we discuss different excited-state methods and their individual drawbacks in detail, one may first want to define a list of properties a theoretical method for excited states should possess beyond the desirable properties for ground-state calculations. In general, a quantum chemical method for the calculation of excited states of large molecular systems should possess the following properties:<sup>[11]</sup>

- 1) The method should treat the electronic ground state and all excited states relevant for the photoinitiated process in a balanced way, thus leading to reliable relative energies.
- 2) The accuracy of the method should allow for direct comparison with experimental data. An error of 0.1–0.2 eV for the excitation energies is desirable, but errors of 0.5 eV are more realistic. Transition moments and excited-state geometries should be reliable and the errors that occur should be predictable.
- 3) The method should be a black-box method yielding reasonable results without a priori knowledge of the system under investigation and without large human effort to set up the calculation.

- 4) The method should be computationally cheap with respect to memory and CPU requirements.

The first two requirements are particularly important for the treatment of excited states of large molecular systems, since their excited states usually lie energetically close together and thus curve crossings are likely. Just these curve crossings are essential for the dynamics of the photoinitiated processes, and knowledge of their occurrence and location is a prerequisite to understand the ongoing processes, especially when optically dark states lie energetically below the initially excited states. For instance, this is the case in carotenoids,<sup>[12]</sup> where the initially excited state ( $S_2$ ) decays usually very fast within 50–200 fs into the lower-lying state ( $S_1$ ), which then determines the dynamics of the photoinitiated process. As a consequence, the relative energies of the states, their oscillator strengths, the shape of their potential energy surfaces, and possible curve crossings must be reliably known, which is only possible if the applied theoretical approach fulfills the requirements (1) and (2).

The requirements (3) and (4) are generally favorable to possess, but they become crucially important if QM/MM schemes for photoinitiated processes are desired. In QM/MM schemes, the dynamics of the photoinitiated process is studied by letting the system evolve in time after the initial excitation, that is, on the potential energy surface of the excited state. The time evolution of the system then requires the repeated calculation of the excited states and their gradients. For a simulation time of 1 ns, approximately 10 000 sequential excited-state calculations need to be performed. This restricts the applicable QM methods to only the computationally cheapest ones, for example semiempirical or approximate DFT methods, which of course are also the least accurate ones. It is also clear that the applied QM method should be a black-box method in a QM/MM scheme, since one wants to avoid tedious manual adjustment of input parameters for that many calculations. Besides easy setup, black-box methods also have the general advantage that the results are independent of a priori knowledge and/or expectation of the researcher.

Today, several quantum chemical approaches for the calculation of excited states and their properties are available. In general they can be divided into three groups: 1) wavefunction-based *ab initio* methods, 2) semiempirical methods, and 3) density functional theory-based approaches. Due to the usually enormous molecular size of biological systems and the need to study large model systems for a meaningful investigation of photoinitiated processes in biological systems, only a few methods remain applicable because of computational limitations. This Minireview is intended to give a brief overview of the most widely used quantum chemical methods for the treatment of excited states of molecular systems of biological interest, that is, of large molecular systems. Therefore the presentation is restricted to the wavefunction-based theories of configuration interaction singles (CIS)<sup>[13,14]</sup> and complete active space self-consistent field (CASSCF),<sup>[15,16]</sup> and to density functional theory-based approaches such as the restricted open-shell Kohn–Sham (ROKS) scheme<sup>[17]</sup> and time-dependent densi-

ty functional theory (TDDFT)<sup>[18–20]</sup> and its variants. In recent years, semiempirical approaches were also successfully applied to the calculation of photoinitiated processes in biological systems, most notably the intermediate neglect of differential overlap (INDO/S) method<sup>[21,22]</sup> in combination with a CIS formalism, and very recently the orthogonalization model 2 (OM2)<sup>[23]</sup> in a multireference configuration interaction (MRCI) framework.<sup>[24,25]</sup> Typical applications of these methods to a few selected biologically relevant systems, for example, rhodopsin, DNA bases, and photosynthetic systems, will be presented.

The Minireview is organized as follows. In Section 2, the basic concepts and mathematical framework of the wavefunction-based methods CIS and CASSCF will be outlined and their properties discussed. Selected applications of CASSCF and also of the more expensive CASPT2 method will be presented, which comprise investigations of the ultrafast photoisomerization of retinal in rhodopsin, of green fluorescent protein and of *p*-coumaric acid in photoactive yellow protein, and of the photoprotection mechanism of DNA bases. In Section 3, semiempirical methods for the calculation of excited states will be introduced and their application to energy-transfer processes in photosynthetic pigments will be highlighted. In Section 4, the density-based ROKS approach, but most notably TDDFT, are presented and their application to energy- and electron-transfer processes in light-harvesting complexes are described. General tools for the analysis of the electronic structure of excited states are described in Section 5. The Minireview concludes with a brief comparison of the described theoretical methods and an outlook on the perspectives of the methods.

## 2. Wavefunction-Based Ab Initio Methods

A wide variety of wavefunction-based ab initio methods exist for the calculation of excited states of molecular systems, which can be divided into single reference and multireference methods on the one hand, and into configuration interaction and coupled-cluster methods on the other. Among these are highly accurate methods such as MRCI approaches,<sup>[26,27]</sup> multireference perturbation theory,<sup>[28–33]</sup> and multireference coupled-cluster (MRCC),<sup>[34,35]</sup> single-reference equation-of-motion coupled-cluster, or linear-response coupled-cluster (EOM-CC, LR-CC) methods.<sup>[36–42]</sup> Closely related to the single-reference coupled-cluster theories is the symmetry-adapted cluster configuration interaction (SAC-CI) approach<sup>[43]</sup> and approximate coupled-cluster schemes of second or third order (CC2, CC3).<sup>[44–47]</sup> A perturbative correction to CIS (see below) is the CIS(D) approach,<sup>[48–50]</sup> which approximately introduces effects of double excitations for the excited states in a noniterative scheme very similar to the Møller–Plesset perturbation theory of second order (MP2), in which doubly excited states are coupled to the ground state. Propagator theories emerging from the Green's function formalism, such as the algebraic diagrammatic construction (ADC) scheme,<sup>[51–54]</sup> also provide an elegant route to the calculation of excited-state properties. Due to their high computational costs, these accurate methods are not applicable to such large molecular systems like those required for the study of photoinitiated processes in biological

systems. Instead, one is essentially restricted to CIS<sup>[13]</sup> and CASSCF<sup>[55]</sup> calculations employing small active spaces and small atomic basis sets. Both methods are frequently applied to the study of photoinitiated processes in biological systems. The basic concepts and working equations of these two methods will be briefly outlined in the following discussion.

A prerequisite of wavefunction-based ab initio calculations of excited states is usually a canonical Hartree–Fock (HF) calculation of the electronic ground state.<sup>[56,57]</sup> The obtained HF ground-state wavefunction  $\Phi_0(r)$  corresponds to the best single Slater determinant describing the electronic ground state of the system. It reads [Eq. (1)]:

$$\Phi_0(r) = ||\phi_1(r)\phi_2(r) \cdots \phi_n(r)|| \quad (1)$$

For simplicity, we assume a closed-shell ground-state electronic configuration and, thus, the  $\phi_i(r)$  correspond to doubly occupied spatial molecular orbitals and  $n=N/2$  ( $N$  is the number of electrons). In general, a HF calculation within a given atomic basis set of size  $K$  yields  $n$  occupied molecular orbitals  $\phi_i(r)$  and  $v=K-n$  virtual orbitals  $\phi_a(r)$ . Here and in the following, we use the indices  $ij,k\dots$  for occupied orbitals,  $a,b,c\dots$  for virtual ones, and  $p,q,r\dots$  for general orbitals.

In configuration interaction-type calculations,<sup>[58]</sup> the electronic many-body wavefunction is constructed as a linear combination of the ground-state Slater determinant and so-called “excited” determinants, which are obtained by replacing occupied orbitals  $\phi_i(r)$  with virtual ones  $\phi_a(r)$ . If only one occupied orbital  $i$  is replaced by one virtual orbital  $a$ , one obtains “singly excited” Slater determinants  $\Phi_i^a(r)$ ; if two occupied orbitals are replaced by two virtual orbitals, one obtains “doubly excited” determinants  $\Phi_{ij}^{ab}(r)$  and so on. The wavefunction then reads [Eq. (2)]:

$$\Psi_{\text{CI}} = c_0\Phi_0(r) + \sum_{ia} c_i^a \Phi_i^a(r) + \sum_{ijab} c_{ij}^{ab} \Phi_{ij}^{ab}(r) + \sum_{ijkabc} c_{ijk}^{abc} \Phi_{ijk}^{abc}(r) \cdots \quad (2)$$

If all possible “excited” determinants are included and this ansatz for the many-body wavefunction is substituted into the exact electronic Schrödinger equation, one arrives at the full CI method, which corresponds to the exact numerical solution of the Schrödinger equation within the chosen atomic basis set. Such calculations are very expensive and at present only feasible with basis sets of good quality for very small systems such as CO, N<sub>2</sub>, CH<sub>4</sub>, or H<sub>2</sub>O. As a consequence, one has to introduce approximations to treat large molecular systems.

The simplest and also crudest approximation is to truncate the CI expansion after the “singly” excited determinants, which yields the CIS ansatz [Eq. (3)]:

$$\Psi_{\text{CIS}} = \sum_{ia} c_i^a \Phi_i^a(r) \quad (3)$$

The ground-state determinant  $\Phi_0(r)$  occurring in Equation (2) vanishes here, since it is uncoupled from the  $\Phi_i^a(r)$  owing to

Brillouin's theorem.<sup>[56]</sup> Substitution of  $\Psi_{\text{CIS}}$  into the molecular Schrödinger equation and projection onto the space of singly excited determinants yields, after some algebra, a matrix equation [Eq. (4)]:

$$\mathbf{H}\mathbf{X} = \omega\mathbf{X} \quad (4)$$

in which  $\mathbf{H}$  is the matrix representation of the Hamiltonian in the space of the singly excited determinants,  $\omega$  is the diagonal matrix of the excitation energies, and  $\mathbf{X}$  is the matrix of the CIS expansion coefficients. The matrix elements of  $\mathbf{H}$  are given as Equation (5):

$$H_{i_a j_b} = (\varepsilon_a - \varepsilon_i) \delta_{ij} \delta_{ab} + (j_a || i_b) \quad (5)$$

where  $\varepsilon_a$  and  $\varepsilon_i$  correspond to the orbital energies of the single-electron orbitals  $\phi_a$  and  $\phi_i$ , respectively, and  $(j_a || i_b)$  corresponds to the antisymmetrized two-electron integrals in standard notation.<sup>[56]</sup>

The excitation energies are finally obtained by solving the following secular equation [Eq. (6)]:

$$(\mathbf{H} - \omega)\mathbf{X} = 0 \quad (6)$$

that is, by diagonalization of the matrix  $\mathbf{H}$ . The obtained eigenvalues correspond to the excitation energies of the excited electronic states, and its eigenvectors to the expansion coefficients according to Equation (3).

Although the CIS ansatz appears to be a rather crude approximation, this method possesses some useful properties. 1) Since CIS is variational, the total energies of ground and excited states correspond to upper bounds to their exact values. 2) The excited-state wavefunctions are properly orthogonal to the ground state. 3) CIS is size consistent. 4) It is possible to obtain pure spin singlet and triplet states for closed-shell molecules by allowing positive and negative combination of  $\alpha$  and  $\beta$  excitations from one doubly occupied orbital. 5) The excited-state energies are analytically differentiable with respect to external parameters as, for example, nuclear displacements and external fields, which makes possible the application of analytic gradient techniques for the calculation of excited-state properties such as equilibrium geometries and vibrational frequencies.<sup>[14,59]</sup> 6) Formally, the computation time scales with  $O(n^4)$  ( $n = n_{\text{occ}} + n_{\text{virt}}$  is the number of basis functions). However, since one is mostly interested only in the energetically lowest excited states, in most implementations the so-called Davidson method is used<sup>[60]</sup> for the diagonalization of the CIS matrix [Eq. (5)], which in practice scales as  $O(n^2)$  to  $O(n^3)$  for larger systems. On today's standard computers this allows for the treatment of fairly large molecules of about 200 first-row atoms comprising about 3500 basis functions.

However, excitation energies computed with the CIS method are usually overestimated, that is, they are usually too large by about 0.5–2 eV compared with their experimental values (see, for instance, refs. [14,61,62]), which makes direct comparison with experimental values difficult. Also the state ordering is sometimes wrong, as for example in polyenes.<sup>[63,64]</sup>

The large error is due to the fact that the energies of the "singly excited" determinants derived from the HF ground state are only very poor first-order estimates for the true excited-state energies, since the virtual orbital energies  $\varepsilon_a$  are calculated for the  $(N+1)$ -electron system instead of for the  $N$ -electron system.<sup>[56]</sup> Consequently, the orbital energy difference  $(\varepsilon_a - \varepsilon_i)$ , which is the leading term in Equation (5), is not related to an excitation energy if the canonical HF orbitals are used as reference. On the other hand, electron correlation is treated in a very unbalanced way within the CIS method. While the electronic ground state remains fully uncorrelated, CIS treats electron correlation of the excited states in an unbalanced way. Although it neglects most parts of the electron correlation and orbital relaxation for the excited states, some singly excited determinants relate to a typical state as single or double excitation, and thus lead to unbalanced correlation of different states. In general, the error can be expected to be the differential correlation energy, which must be at least on the order of the correlation energy of one and sometimes several electron pairs. Such energies are typically on the order of 1 eV per electron pair, and hence one should expect errors of this magnitude. The wrong order of states is mostly owing to the neglect of doubly and higher excited determinants in the CI expansion [Eq. (2)], since doubly excited states can be important in the low-energy region of the electronic spectrum, and those are not included in CIS.

Today, CIS is practically no longer employed for the calculation of excited states, and it is mostly substituted by TDDFT when large molecules are studied, or by more sophisticated wavefunction-based approaches when medium-sized or small molecules are investigated. As we will see later, TDDFT yields fairly accurate results for valence excited states but exhibits substantial problems, in particular with charge-transfer (CT) excited states. On the contrary, CT excited states are reasonably well described within CIS, and thus CIS constitutes a viable approach to gain insight into whether charge-transfer excited states are relevant to the problem of interest. Also, CIS can be used to obtain asymptotically correct potential energy surfaces for CT excited states with respect to charge separation coordinates.

Another possibility to restrict the CI ansatz [Eq. (2)] is not to limit the excitation level of the determinants, but to restrict the molecular orbitals from which and to which electrons should be excited. In other words, one can define an active space of occupied and virtual orbitals in which all possible "excited" determinants are constructed, that is, in which a full CI calculation shall be performed (Figure 1). Since such an approximation is a severe limitation of the flexibility of the CI wavefunction, it usually leads to substantial errors, and one has to reoptimize the molecular orbitals during the minimization procedure to improve the accuracy. Loosely speaking, one couples the self-consistent HF-like scheme with the CI formalism, and thereby one obtains a set of nonlinear multiconfiguration self-consistent field (MCSCF) equations, which need to be solved in an iterative manner until self-consistency is reached. The definition of an active space as in Figure 1, in which the full CI expansion is performed, gives the most widely used

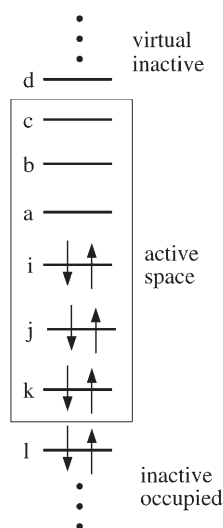


**Figure 1.** Pictorial scheme of the definition of an active space as required in CASSCF theory. The chosen orbital selection would correspond to a six-electrons-in-six-orbitals (6,6) CASSCF calculation.

wavefunction-based method for large molecules its name: complete active space self-consistent field (CASSCF).<sup>[55,57]</sup>

In analogy to CIS, CASSCF is variational, size-consistent, and possesses all the positive properties of CIS. The size-consistency of CASSCF, however, is only achieved when the CASSCF space is properly chosen, which in practice is often impossible. Also, analytical derivatives are available allowing for efficient optimization of excited-state geometries and localization of conical intersections.<sup>[65–67]</sup> However, from a computational point of view, CASSCF calculations become very quickly very expensive, since the computational effort increases exponentially with the size of the active space. At present, active spaces with 12 electrons in 12 orbitals constitute the computationally feasible limit<sup>[11]</sup> for small molecules, and thus for large molecules one is usually confined to smaller active spaces. The computational cost for the orbital optimization step is roughly the same as that for a CIS calculation. In general, the accuracy of CASSCF calculations strongly hinges on the size of the chosen active space and the quality of the atomic basis set. For the investigation of photoinitiated processes in biological systems, the active space is usually chosen as large as necessary and as small as possible to find a good compromise between computational effort and accuracy, typically containing six electrons in six orbitals. This results in errors in the excitation energies of about 0.5 to 1.0 eV.

However, three general problems exist with CASSCF calculations. Firstly, one has to choose for which state the orbitals are to be optimized. Unfortunately, this choice is not unique but has an influence on the relative energies of the calculated excited states and can even change their energetic ordering. One way to partially circumvent this problem is to perform a state-averaged CASSCF calculation, in which the orbitals are optimized with respect to a weighted mean of all states of interest. Secondly, the choice of the active space is not unique as well, and requires first and foremost a careful consideration of the

processes to be studied and a priori knowledge of the relevant orbitals. An unbalanced choice of active orbitals will lead to an unbalanced treatment of the excited states. For example, if the chosen active space consists only of  $\pi$  and  $\pi^*$  orbitals of an unsaturated molecule, the calculated spectrum will contain only  $\pi\pi^*$  excited states. Other states, for instance  $n\pi^*$  states, will not be found, although in general they cannot a priori be excluded, since they might become important in the course of the studied photoinitiated process. In principle, one has to increase the active space successively until the excited states of interest are converged, which unfortunately is in most cases computationally not feasible, and very often the employed active spaces are far from being converged. Thirdly, too small active spaces and the concomitant neglect of large parts of dynamical electron correlation can lead to significant errors and an unbalanced treatment of different classes of electronic states, since states with different electronic structures can exhibit varying degrees of electron correlation.

A very successful approach to correct for the missing dynamic electron correlation is second-order perturbation theory building up on the CASSCF wavefunctions (CASPT2) already mentioned above.<sup>[29–31]</sup> In general, one performs a state-averaged CASSCF calculation first, in which the orbitals are optimized for an averaged state vector consisting of an equally weighted sum of the electronic states of interest. Thereby, a balanced molecular orbital basis is obtained for the subsequent perturbation theory calculation. Very often this procedure leads to an improved description of the excited states, and indeed CASPT2 has proven to give quantitative results for small molecules. However, if the amount of neglected dynamic correlation is a significant part of the total dynamic correlation, which is usually the case for larger molecules, then second-order perturbation theory cannot be sufficient to correct for the introduced imbalances.

CASSCF and CASPT2 calculations have been successfully employed to study the first events in photoinitiated processes in many biological systems with not-too-large photoactive pigments. Such calculations contributed largely to the understanding of, for example, the ultrafast photoisomerization of retinal, the photoactive pigment of rhodopsin that is responsible for vision. It is well-known that retinal in rhodopsin undergoes an 11-*cis*  $\rightarrow$  *all-trans* isomerization upon photoexcitation within 200 fs, which leads to the signaling state of the protein.<sup>[68]</sup> CASSCF calculations revealed that the isomerization proceeds via a conical intersection between the first excited  $S_1$  state and the electronic ground state, which explains the ultrafast reaction and gives an atomistic model for the isomerization mechanism.<sup>[69–71]</sup> A conical intersection can be understood as a photochemical funnel that allows for ultrafast transitions between electronic states and concomitantly ultrafast photoreactions.<sup>[72,73]</sup> Recent calculations on retinal model systems<sup>[74–76]</sup> and on the real system including the protein environment<sup>[77]</sup> could give an explanation for the acceleration of the isomerization of 11-*cis*-retinal in the protein compared to retinal in the gas phase. The effect of the counterion on the photoinitiated isomerization has been studied,<sup>[78–80]</sup> and the origin of the bathochromic shift in the early photointermediates of the rho-

dopsin photocycle has been investigated by employing CASSCF calculations.<sup>[81]</sup>

Recently, a special hybrid QM/MM force field was developed for studying the retinal chromophore in rhodopsin that couples CASPT2 single-point calculations at CASSCF geometries for retinal with the Amber force field for the rest of the protein.<sup>[80]</sup> This new QM/MM scheme was employed to study the counterion effect on the isomerization of retinal in rhodopsin and bacteriorhodopsin.<sup>[82]</sup> It was demonstrated that the counterion influences the relative stability of the relevant excited states, introduces reaction barriers along reaction paths different from the 11-*cis*→*all-trans* isomerization, and furthermore changes the nature of the decay funnel. The excited-state structures, the spectral fine-tuning by the environment, and the spectroscopy of the retinal chromophore have also been addressed.<sup>[83–86]</sup> A quantum dynamics investigation using CASSCF/CASPT2 potential energy surfaces revealed that small barriers on excited-state surfaces can induce a multiexponential decay of the photoexcited retinal chromophore.

Similarly, CASSCF/CASPT2 methodology has been employed to study the photoinitiated processes in the famous green fluorescent protein (GFP), which is widely used in molecular biology to stain living cells. Elaborate gas-phase model calculations allowed the identification of an efficient radiationless decay channel in the gas phase, which is hampered in the native protein environment.<sup>[87,88]</sup> Inclusion of the environment by a QM/MM simulation revealed that the counterion effect is only small and that the charges of the protein backbone seem to compensate its effect.<sup>[89]</sup>

A similar example for the successful application of CASSCF is the investigation of the photocycle of the photoactive yellow protein (PYP), which is the primary photoreceptor for the negative phototactic response of the bacterium *Halorhodospira halophila*.<sup>[90]</sup> Upon photoexcitation, the *p*-coumaric acid chromophore of PYP undergoes an ultrafast photoisomerization from the *trans* to the *cis* configuration similar to retinal in rhodopsin (Figure 2). CASSCF calculations clearly revealed that the

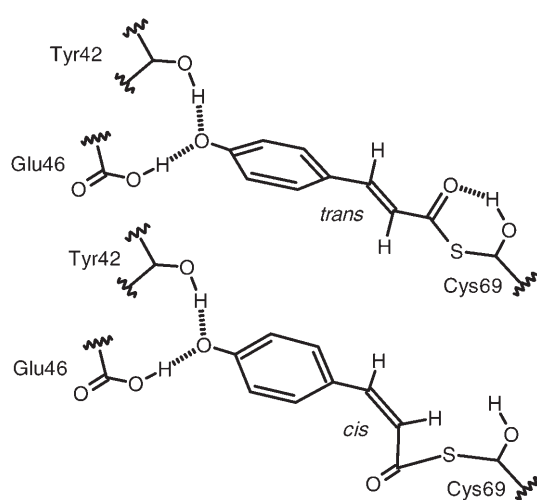


**Figure 2.** Molecular structure of the *p*-coumaric acid chromophore in PYP in the ground state and after absorption and photoisomerization according to ref. [91].

isomerization in PYP is also mediated by a conical intersection.<sup>[91–94]</sup> The influence of the protein environment was studied by a QM/MM approach, in which (6,6)-CASSCF calculations with a 3-21G basis set were used to model the excited-state dynamics of the chromophore quantum mechanically. It was shown that the protein stabilizes the  $S_1$  excited state of the chromophore, and as a consequence the relevant  $S_1/S_0$  conical intersection is moved into a position that is faster and more efficiently reached compared to the free molecule, thus allowing for a very efficient photoinitiated isomerization process in the protein.<sup>[91]</sup>

One last example of the application of CASSCF calculations to photoinitiated processes in biological systems is the investigation of the ultrafast photodynamics of DNA bases upon irradiation with UV light. By employing mainly CASSCF-based calculations, it has been shown that DNA bases can undergo rapid, radiationless deactivation via hydrogen predissociation.<sup>[95]</sup> The detailed mechanism is based on a  $\pi\sigma^*$  state that is repulsive along the H-abstraction coordinate and that intersects the initially excited  $\pi\pi^*$  and  $n\pi^*$  states as well as the electronic ground state.<sup>[95–98]</sup> It is believed that this process is the main mechanism of how DNA is protected against UV irradiation.<sup>[96,99]</sup> The photochemistry of different isomers of DNA bases has also been studied by employing a hybrid approach consisting of DFT and multireference CI.<sup>[100]</sup> A conical intersection between the first excited state and the ground state of cytosine could be identified for the keto isomer and ketoimine tautomer, thus explaining the short observed excited-state lifetimes of these species.<sup>[101]</sup> In combined experimental and theoretical studies such calculations contributed largely to the understanding of the excited-state dynamics of 2-aminopurine and protonated adenine.<sup>[102,103]</sup>

### 3. Semiempirical Molecular Orbital Theories

During the last few years, semiempirical methods have frequently been used for the theoretical investigation of large biological systems, which was largely triggered by the need for theoretical support in the interpretation of experimental data. The reason for the success of semiempirical methods lies in their small computational demands, which allows for an approximate quantum mechanical treatment of very large molecular systems, and in the lack of more reliable alternatives for such large systems. The gist of semiempirical molecular orbital theories is to substantially reduce the computational cost of wavefunction-based *ab initio* theories by introducing chemically virtuous approximations.

At the heart of semiempirical methods lies the approximation of the one- and two-electron integrals that need to be calculated explicitly prior to an *ab initio* HF calculation, which is usually the starting point for excited-state approaches (see Section 2). In general, the one- and two-electron integrals are given in the atomic orbital basis as the matrices **I** and **II**, respectively, which are defined as Equations (7) and (8):

$$(\mathbf{I})_{\mu\nu} = \sum_{\mu\nu} \int \chi_{\mu}^*(r) \hat{h}(r) \chi_{\nu}(r) dr \quad (7)$$

$$(\mathbf{II})_{\mu\nu\lambda\sigma} = \sum_{\mu\nu\lambda\sigma} \int \int \frac{\chi_{\mu}^*(r_1) \chi_{\nu}(r_1) \chi_{\lambda}^*(r_2) \chi_{\sigma}(r_2)}{|r_1 - r_2|} dr_1 dr_2 \quad (8)$$

where the  $\{\chi_{\mu}\}$  correspond to the chosen atomic basis functions,  $\hat{h}(r)$  is the core Hamiltonian containing the kinetic energy of the electrons and the electron–nucleus attraction, and the indices run over all atomic basis functions. Calculation of the matrix  $\mathbf{II}$  is especially computationally demanding, since it corresponds to a four-index quantity and scales thus formally with  $O(n^4)$  ( $n$  being the number of atomic basis functions). Analysis of the matrix elements of  $\mathbf{II}$  reveals that many of them are close to zero, which allows for the introduction of various approximations.

To illustrate the spirit of semiempirical approaches, one of the easiest methods, the complete neglect of differential overlap (CNDO) method,<sup>[104,105]</sup> will be briefly described. In this method one Slater-type atomic basis function is employed for each atomic valence orbital and as the name of the method already indicates, differential overlap between different basis functions is generally neglected [Eq. (9)]:

$$S_{\mu\nu} = \int \chi_{\mu}^*(r) \chi_{\nu}(r) dr = \delta_{\mu\nu} \quad (9)$$

where  $\delta$  is the Kronecker delta. All two-electron integrals  $(\mathbf{II})_{\mu\nu\lambda\sigma}$  are parameterized in the following way [Eq. (10)]:

$$(\mathbf{II})_{\mu\nu\lambda\sigma} = \delta_{\mu\nu} \delta_{\lambda\sigma} (\mathbf{II})_{\mu\mu\lambda\lambda} \quad (10)$$

that is, only matrix elements are considered between pairs of identical basis functions, where each pair is located on one atom. The two pairs, however, do not necessarily need to be located on the same atom. If  $\chi_{\mu}$  and  $\chi_{\lambda}$  are located on the same atom A, the corresponding integral can be approximated using the Pariser–Parr approximation [Eq. (11)]:<sup>[106]</sup>

$$(\mathbf{II})_{\mu\mu\lambda\lambda} = IP_A - EA_A \\ = \pi_{AA} \quad (11)$$

where  $IP_A$  and  $EA_A$  correspond to the experimental ionization potential and electron affinity of atom A, respectively. Integrals between function pairs on different atoms can be estimated via Equation (12):

$$\pi_{AB} = \frac{\pi_{AA} + \pi_{BB}}{2 + r_{AB}(\pi_{AA} + \pi_{BB})} \quad (12)$$

where  $r_{AB}$  is the distance between atoms A and B.<sup>[107]</sup> The one-electron integrals are within the CNDO method approximated as Equations (13) and (14):

$$(\mathbf{I})_{\mu\mu} = -IP_A - \sum_K (Z_K - \delta_{Z_A Z_K}) \pi_{AK} \quad (13)$$

$$(\mathbf{I})_{\mu\nu} = \frac{(\beta_A + \beta_B) S_{\mu\nu}}{2} \quad (14)$$

where orbital  $\chi_{\mu}$  is located on atom A and  $\chi_{\nu}$  on B.  $Z$  refers to the nuclear charge of the corresponding atom, and  $\beta$  is a resonance parameter describing the strength of interaction between atoms. Note that the overlap matrix  $\mathbf{S}$  contained in Equation (14) is different from that defined in Equation (9). The  $\beta$  parameters contained in Equation (14) are usually adjusted such that the method reproduces certain experimental quantities. The introduced severe approximations reduce the computational cost from  $O(n^4)$  for ab initio HF calculations to only  $O(n^2)$  for CNDO.

However, due to the severe approximations, CNDO is not a reliable method for the calculation of molecular properties. Improvements of the simple CNDO scheme are achieved by lifting the constraints for the two-electron integrals [Eq. (10)] and allowing for different values for the integrals for different basis function types. This re-parameterization yields the INDO method,<sup>[108]</sup> which exhibits reasonable accuracy for molecular ground-state properties. The INDO/ $S^2$  model is specifically optimized for spectroscopic properties,<sup>[21,22]</sup> that is, excited states, and is thus regularly used as a starting point for CIS-type calculations (see Section 2). The simple structure of the one- and two-electron integrals allows for an efficient and fast computation of excited states of very large molecular systems. The accuracy of the method, however, is unpredictable, and careful comparison with experiment and/or higher-level computations must be made, if possible.

Among many other applications, excited-state calculations based on the INDO/S model have been employed to study energy-transfer processes in light-harvesting complexes and reaction centers of the photosynthetic apparatus of purple bacteria and plants. For example, the solution of the structure of the light-harvesting complex (LH2) of *Rhodospseudomonas acidophila* and *Rhodospirillum molischianum*<sup>[109,110]</sup> revealed that they contain two ring structures with nine or eight weakly coupled and 18 or 16 strongly coupled B800 and B850 bacteriochlorophylls (BChls), respectively (Figure 3). This immediately poses the questions as to whether the low-lying excited states of these coupled rings are localized on individual BChls or whether they are delocalized over several, and what the underlying mechanism of excitation energy transfer (EET) might be. Early INDO/S-CIS calculations have been used to study energy-transfer dynamics and they predicted the low-lying excitonic states to be distributed essentially over all BChls.<sup>[111,112]</sup> The calculated rates for EET were in excellent agreement with experimental data. Calculations with a localized-density-matrix method based on the INDO/S model Hamiltonian largely corroborated these findings, and gave evidence that the low-lying excited state in the strongly coupled B850 ring is distributed over at least five neighboring BChl molecules.<sup>[113,114]</sup> In the latter investigation, the excitation energies of the  $Q_y$  state of BChl were underestimated by approximately 0.5 eV; however, this at first glance large error does not play a crucial role when

<sup>2</sup> While INDO is the method, that is, body of formulas, INDO/S is a model, since it refers to a specific set of parameters used within an INDO calculation.

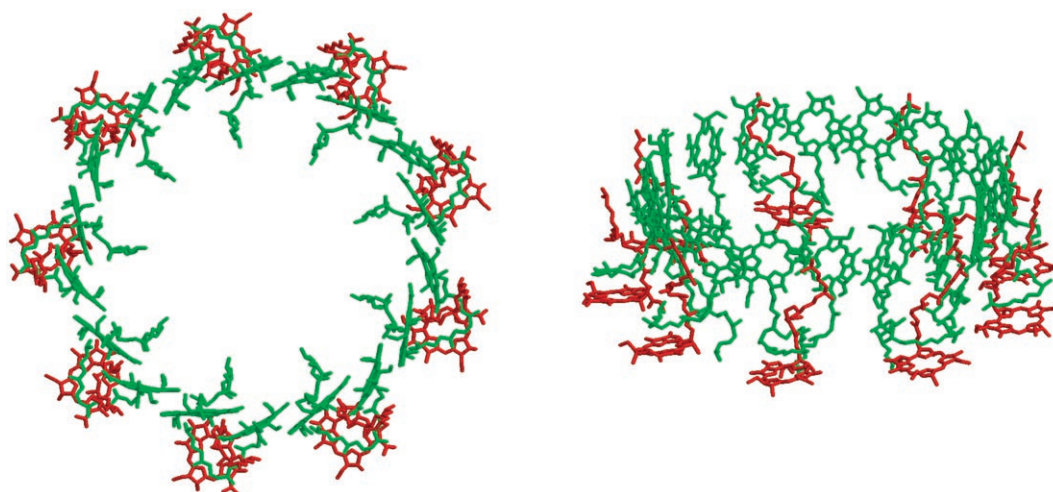


**Figure 3.** Molecular arrangement of the weakly coupled B800 ring (red) and the strongly coupled B850 ring (green) in the light-harvesting complex (LH2) of *Rhodospseudomonas acidophila*.

describing the EET dynamics, since the same error is made for all relevant states such that the error basically cancels completely.

Similarly, the excitation energy-transfer dynamics of chlorophyll excitations in photosystem I of *Synechococcus elongatus* have been modeled with an effective excitonic Hamiltonian, after the excitation energies of all present 96 chlorophyll molecules and couplings between spatially close pairs had been calculated with the INDO/S-CIS approach.<sup>[115]</sup> This procedure allowed a tentative assignment of red chlorophylls and the calculation of the absorption spectrum of the whole photosystem I. Furthermore, a detailed study of the electronic couplings and energy-transfer dynamics in the oxidized primary electron donor of the bacterial photosynthetic reaction center that employed INDO/S-MRCI calculations unraveled the mechanism of EET from neighboring accessory BChls to the oxidized special pair.<sup>[116]</sup>

Another successful semiempirical method is the neglect of diatomic differential overlap (NDDO) method which, in comparison with the INDO method, allows a more flexible parameterization of one-center two-electron integrals [Eq. (10)] and also improves the two-center two-electron integrals. In this context, a new NDDO-based semiempirical method has recently been proposed that is called orthogonalization model 2 (OM2).<sup>[23]</sup> It has been recognized that the neglect of all three- and four-center two-electron integrals [Eq. (10)] is only then a justified approximation if the atomic basis functions are orthogonal.<sup>[117–119]</sup> Within OM2, corrections have been included that correct for valence-shell orthogonalization effects on the resonance integrals and on repulsive core–valence interactions. It is hoped that the inclusion of orthogonalization effects cures some of the most dramatic failures of previous semiempirical theories.<sup>[23]</sup> Recently, an MRCI scheme based on the OM2 model Hamiltonian has been implemented,<sup>[24,25]</sup> which allows for the calculation of excited electronic states. It is expected that the inclusion of orthogonalization effects and the concomitant increase of the occupied–virtual gap of the orbitals

also improves the accuracy of excited-state calculations, since excitation energies were typically underestimated by previous semiempirical models.<sup>[120]</sup> First calculations on small molecules do indeed look promising,<sup>[25]</sup> but a thorough evaluation of the model is still required.

#### 4. Density Functional Theory-Based Approaches

Ground-state DFT has the same role in excited-state calculations within the DFT framework as HF calculation has in wavefunction-based excited-state methods. Similar to the HF method, DFT yields molecular orbitals and orbital energies, which serve as a starting point for further excited-state calculations. DFT in the Kohn–Sham formulation (KS-DFT) relies on the Hohenberg–Kohn (HK) theorems<sup>[121]</sup> and the existence of a noninteracting reference system, whose electron density equals that of the real system<sup>[122]</sup> (for reviews in the field of ground-state DFT, the reader is referred to refs. [8,9,123,10,124]).

In principle, ground-state DFT calculations can be tweaked to calculate a particular electronically excited state by introduction of constraints. These constraints may be, for example, a different spin multiplicity than the ground state, or equally well, the excited state of interest may belong to a different irreducible representation of the molecular point group. Following this procedure, excited-state properties such as equilibrium geometries and static electric moments are accessible. The excitation energy is given as the difference of the total energies of the electronic ground state and the excited state obtained in two independent calculations. This method is also commonly referred to as the  $\Delta$ SCF method,<sup>[125]</sup> but the methodology can be applied with any ground-state method. Logically, this approach breaks down if one is interested in excited states of the same spin multiplicity and same irreducible representation of the spatial symmetry group as that of the electronic ground state. This is particularly often the case if one wishes to study

photoinitiated processes in biological systems, since large molecular models mostly do not exhibit any spatial symmetry.

A similar approach is the ROKS method,<sup>[17,126–128]</sup> which allows the computation of the lowest excited singlet state even if it belongs to the same irreducible representation as the electronic ground state. It is closely related to the restricted open-shell HF method for the low-spin case,<sup>[129]</sup> and relies on the idea that the energy of the lowest singlet state can be extracted from the energy of the HOMO→LUMO singly excited Slater determinant in singlet and triplet configuration (Figure 4). It is apparent from Figure 4 that the energy of the lowest singlet state is simply given as Equations (15) and (16):

$$E^{\text{sing}} = 2E_S^{\text{sing}} - E_S^{\text{trip}} \quad (15)$$

$$E^{\text{sing}} = 2\langle \Phi_S^{\text{sing}} | \hat{F}^{\text{KS}} | \Phi_S^{\text{sing}} \rangle - \langle \Phi_S^{\text{trip}} | \hat{F}^{\text{KS}} | \Phi_S^{\text{trip}} \rangle \quad (16)$$

Minimization of the energy expression (16) with respect to the molecular orbitals  $\phi_p(r)$  constituting the Slater determinants  $\Phi_S$  and  $\Phi_T$  yields the ROKS scheme comprising two sets of nonlinear differential equations, one for the doubly occupied orbitals

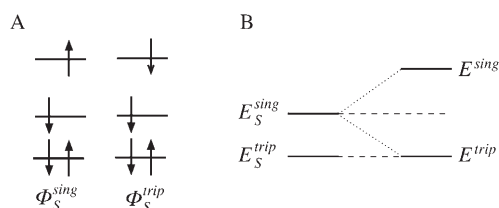


**Figure 4.** A) Relevant singly excited determinants for the ROKS scheme. B) Energies of the singly excited determinants compared with the energies of the singlet and triplet states.

and one for the singly occupied orbitals. Thereby the energy of the spin-adapted singlet state, the linear combination of two singly excited determinants, is obtained. The equations can either be solved by iterative diagonalization or direct minimization, the latter of which is particularly useful for implementations of ROKS in a Car–Parinello molecular dynamics (CPMD) framework.<sup>[17,130]</sup> However, since ROKS always yields only the lowest singlet excited state, it is not possible to calculate the complete electronic spectrum. Also, doubly excited states are not included in the method, which may well be relevant for large molecular systems. Recently, ROKS has been applied in a QM/MM scheme to study the ultrafast isomerization of retinal in its binding pocket in rhodopsin.<sup>[131]</sup> Although at ambient temperatures no photoisomerization could be observed, ultrafast isomerization was obtained when the local temperature was artificially increased to 690 K. Then, it could be shown that no atom of the retinal had to move more than 0.8 Å to perform the isomerization from the 11-*cis* to the *all-trans* form of retinal.

Today, the most widely used theoretical method to investigate electronically excited states of medium-sized to large molecular systems is linear-response time-dependent functional theory (TDDFT). The Runge–Gross theorems<sup>[18]</sup> and their extensions<sup>[132,133]</sup> have led to the formulation of the so-called time-dependent Kohn–Sham equations [Eq. (17)]:

$$i \frac{\partial}{\partial t} \phi_i(r, t) = \hat{F}^{\text{KS}}(r, t) \phi_i(r, t) \quad (17)$$

which yield the time-dependent one-particle density according to Equation (18):

$$\rho(r, t) = \sum_i^{n_{\text{occ}}} |\phi_i(r, t)|^2 \quad (18)$$

In the above equations,  $\phi_i(r, t)$  correspond to time-dependent occupied molecular orbitals and  $\hat{F}^{\text{KS}}(r, t)$  is the time-dependent Kohn–Sham operator. For more details on formal aspects of the derivation of the time-dependent Kohn–Sham equations, the reader is referred to refs. [19, 20, 133, 134].

Two different strategies can be followed to obtain excitation energies and oscillator strengths employing the time-dependent Kohn–Sham approach. One possibility is to propagate the time-dependent Kohn–Sham wavefunction in time, which is referred to as real-time TDDFT.<sup>[135,136]</sup> This technique still has the status of an expert’s method but it is beginning to be used in chemistry and biophysics, and some successful applications have been reported recently in the literature.<sup>[137,138]</sup> The other possibility for obtaining excited-state properties is to analyze the linear response of the time-dependent Kohn–Sham equations with respect to an external oscillating electric field, which yields the linear-response TDDFT equations. If one speaks of TDDFT today, one usually refers to the latter linear-response TDDFT approach. The key steps of its derivation will be briefly outlined in the following discussion.

The basic idea is to apply time-dependent perturbation theory to first order and to describe the time-dependent linear response of the one-particle density to a time-dependent oscillating electric field. Before the time-dependent electric field is applied, the molecular system is assumed to be in its electronic ground state, that is, to obey the ground-state Kohn–Sham equation [Eq. (19)]:

$$\hat{F}^{\text{KS},0}(r) \Phi_0^{\text{KS}} = E_0^{\text{KS}} \Phi_0^{\text{KS}} \quad (19)$$

with [Eq. (20)]:

$$\rho^0(r) = \sum_i^{n_{\text{occ}}} |\phi_i(r)|^2 \quad (20)$$

where  $\hat{F}^{\text{KS},0}(r)$  is the time-independent Kohn–Sham operator,  $\Phi_0^{\text{KS}}$  the ground-state Kohn–Sham Slater determinant,  $\phi_i(r)$  the occupied Kohn–Sham orbitals, and  $E_0^{\text{KS}}$  the corresponding ground-state total energy. Now a time-dependent oscillating electric field of the form [Eq. (21)]:

$$E(t) = fe^{i\omega t} + f^*e^{-i\omega t} \quad (20)$$

is applied, and as a consequence the Kohn–Sham orbitals, the electron density, and the Kohn–Sham operator will change, since the latter depends itself on the orbitals. The applied field is a small perturbation, and therefore the new density can in first order be written as Equation (22):

$$\rho(r,t) = \rho^0(r) + \delta\rho(r,t) \quad (22)$$

and the time-dependent Kohn–Sham operator takes on the following appearance [Eq. (23)]:

$$\hat{F}^{\text{KS}}(r,t) = \hat{F}^{\text{KS},0}(r) + \left[ \frac{\delta \hat{F}^{\text{KS},0}}{\delta \rho(r)} \right]_{t=t_0} \delta\rho(r,t) + E(t) \quad (23)$$

where the second term on the right-hand side corresponds to the linear change of the ground-state Kohn–Sham operator  $\hat{F}^{\text{KS},0}(r)$  when the perturbation is switched on. Substitution of Equations (22) and (23) into Equation (16), collection of all first-order terms, and careful analysis of orthogonality constraints yields, after Fourier transformation into the energy space, the TDDFT equation for the excitation energies and transition vectors (see, for example, refs. [19,20,139,140]). In compact matrix notation, the TDDFT equations read [Eq. (24)]:

$$\begin{pmatrix} \mathbf{A} & \mathbf{B} \\ \mathbf{B}^* & \mathbf{A}^* \end{pmatrix} \begin{pmatrix} \mathbf{X} \\ \mathbf{Y} \end{pmatrix} = \omega \begin{pmatrix} \mathbf{1} & \mathbf{0} \\ \mathbf{0} & -\mathbf{1} \end{pmatrix} \begin{pmatrix} \mathbf{X} \\ \mathbf{Y} \end{pmatrix} \quad (24)$$

where the matrix elements are given for a hybrid exchange–correlation (xc) functional as Equations (25) and (26):

$$A_{ia,jb} = \delta_{ij}\delta_{ab}(\varepsilon_a - \varepsilon_i) + (ja|ib) - c_{\text{HF}}(ji|ab) + (1 - c_{\text{HF}})(ja|f_{\text{xc}}|ib) \quad (25)$$

$$B_{ia,jb} = (ja|bi) - c_{\text{HF}}(jb|ai) + (1 - c_{\text{HF}})(ja|f_{\text{xc}}|bi) \quad (26)$$

Equation (24) is a non-Hermitian eigenvalue equation, the solution of which yields excitation energies  $\omega$  and transition vectors  $|XY\rangle$  determining the first-order change in the density and thereby also the excited-state wavefunction. Although the exchange–correlation kernel  $f_{\text{xc}}$  of Equations (25) and (26) is formally energy-dependent, in practical calculation standard ground-state xc functionals, for instance SVWN,<sup>[141,142]</sup> BLYP,<sup>[143,144]</sup> PBE,<sup>[145,146]</sup> or B3LYP,<sup>[147]</sup> are employed to evaluate those terms. This is a consequence of the so-called adiabatic local density approximation (ALDA), which requires that [Eq. (27)]:

$$f_{\text{xc}}(\omega, r, r') = f_{\text{xc}}(r)\delta(r - r') \quad (26)$$

Notably, Equation (24) contains four different but closely related schemes for the calculation of excited states (Figure 5).<sup>[20]</sup> If the coefficient  $c_{\text{HF}}$  which measures the amount of nonlocal HF exchange in the xc functional, is equal to 1.0 in Equations (25) and (26), the scheme reduces to the well-known time-dependent Hartree–Fock (TDHF) scheme.<sup>[148–152]</sup> If the

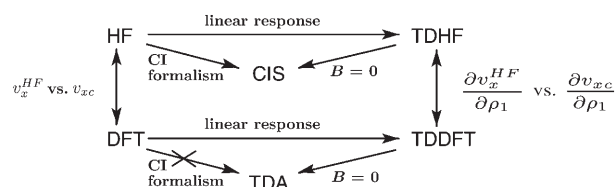


**Figure 5.** Schematic diagram of the relation between HF and DFT, and time-dependent Hartree–Fock (TDHF) and time-dependent DFT (TDDFT), as well as configuration interaction singles (CIS) and the Tamm–Dancoff approximation (TDA) to TDDFT.

Tamm–Dancoff approximation (TDA) is performed, which means that the  $\mathbf{B}$  matrix is neglected in Equation (24), one arrives in the case of TDDFT ( $c_{\text{HF}} \neq 1.0$ ) at the TDA/TDDFT scheme<sup>[139]</sup> and in the case of TDHF ( $c_{\text{HF}} = 1.0$ ) at CIS. The latter becomes clear if Equations (24) and (25) with  $\mathbf{B} = 0$  and  $c_{\text{HF}} = 1.0$  are compared with Equations (4) and (5) in Section 2. Hence, there exist two routes to the CIS scheme: one is via the CI formalism as presented previously, and the other is via linear response theory. An approach that combines ground-state DFT with CIS has been proposed previously,<sup>[153]</sup> in which CIS computations according to Equation (4) are performed with shifted Kohn–Sham orbital energies and empirically scaled Coulomb-type two-electron integrals (second term on the right-hand side of Equation (5)). A tight-binding approach to TDDFT, the so-called TDDFTB method, has also been developed, which decreases the computational effort further.<sup>[154]</sup>

The computational expense of TDDFT calculations scales approximately like  $O(n^3)$  and additional computation time can be saved by a factor of 3–8 depending on the system of interest if the resolution-of-the-identity (RI) approximation<sup>[155]</sup> is used to evaluate the Coulomb-like terms of Equations (25) and (26).<sup>[156,157]</sup> On a modern computer, molecular systems with up to 2000 basis functions (approximately 150 first-row atoms) can be treated by TDDFT in the standard implementation, and systems with up to 4500 or so basis functions (300 atoms) can be reached by TDDFT when the RI approximation is used.

For valence excited states, for example  $\pi\pi^*$ ,  $n\pi^*$ , or  $no^*$  states, whose excitation energies are well below the ionization potential, TDDFT exhibits an accuracy similar to that of sophisticated wavefunction-based methods of approximately 0.2–0.8 eV depending on the system. Very often these excited states are slightly shifted in energy by an almost constant value compared with the experimental electronic absorption spectrum, but the relative energies between the states are reproduced very favorably (see, for example, refs. [95,158,159]). Despite the success of TDDFT for valence excited states, it exhibits substantial errors for the calculation of Rydberg excited states, doubly excited states,<sup>[160,161]</sup> ionic states of systems with large  $\pi$  systems,<sup>[162,163]</sup> and charge-transfer excited states,<sup>[164–167]</sup> which are all well documented today.<sup>[20]</sup> Particularly, the three latter problems prevent TDDFT from being a black-box method for excited states, and instead they always demand a careful examination of the calculated excited states and expert knowledge. Nevertheless, if these failures can be cured, TDDFT possesses the potential to become a viable approach to be employed for large systems and/or in QM/MM schemes, since

then the method possesses all the requirements 1)–4) outlined in the Introduction. It can yield reliable relative energies with reasonable absolute accuracy, it will be a black-box method, and the computational effort is relatively small.

In recent years, analytic gradients have been presented for the excited states,<sup>[168–170]</sup> which makes the efficient calculation of excited-state properties like equilibrium geometries and dipole moments with TDDFT possible. The calculated properties for the excited states can be expected to be of the same quality as those calculated with standard KS-DFT for the ground state, if the studied state does not belong to one of the classes of states mentioned above, for which TDDFT fails. In combination with numerical calculation of the harmonic frequencies, it has been shown that TDDFT can reproduce vibrationally resolved electronic spectra of medium-sized organic molecules with reasonable accuracy and allows for an assignment of spectral features.<sup>[171,172]</sup>

The application of TDDFT to photoinitiated processes in biological systems is tedious due to the failures mentioned above, which are particularly dramatic for large molecules or aggregated systems, both being typical for biological systems. Most notably, the failure for CT excited states leads to spurious states in the low-energy region.<sup>[164,167,173]</sup> A first and helpful test of the applicability of TDDFT is the investigation of the dependence of the results on the xc functional. If, for instance, a local functional (SVWN), a gradient-corrected functional (BLYP, BP86), and a hybrid functional (B3LYP) yield substantially different results for the excited states, one should not rely on TDDFT for the investigation, whereas if the results are essentially independent of the xc functional, the system can well be treated with TDDFT. However, if possible, results from TDDFT calculations should always be compared with experimental data or calculations on higher levels of theory.

A very promising ansatz for the treatment of CT states is the inclusion of nonlocal HF exchange at long-range electron–electron interaction, which has been realized in a couple of schemes so far.<sup>[174–176]</sup> In all these schemes, the Coulomb operator of the Hamiltonian is split up into two parts, a short-range and a long-range part, as for example in ref. [174] [Eq. (28)]:

$$\frac{1}{r_{12}} = \frac{1 - \text{erf}(\mu r_{12})}{r_{12}} + \frac{\text{erf}(\mu r_{12})}{r_{12}} \quad (28)$$

where  $r_{12} = |r_1 - r_2|$ . The first term on the right-hand side corresponds to the short-range part and is evaluated using the xc potential from DFT, while the second term, the long-range part, is calculated with exact HF exchange. This idea is fairly old and was originally suggested by Stoll and Savin in 1985.<sup>[177–180]</sup> The scheme [Eq. (28)] has been applied in combination with various xc functionals to yield, for instance, LC-BLYP, which indeed corrects the failures of TDDFT for CT excited states.<sup>[174]</sup> A major drawback of this approach, however, is that the standard xc functionals require a refitting procedure. Similar in spirit is the approach of Baer and Neuhauser, who also include long-range HF exchange but who employ a different partition function for the Coulomb operator.<sup>[176]</sup> An extension of this approach has been presented by Yanai et al. who

combine B3LYP<sup>[147]</sup> at short range with an increasing amount of exact HF exchange at long range, which results in a functional called CAM-B3LYP<sup>[175]</sup> that gives excellent CT excitation energies in comparison with benchmark calculations. However, since they use at long range 60% HF exchange at most, the long-range asymptotic behavior of the CT states is not fully corrected.<sup>[175]</sup> A slightly different route is taken by Griessenko and Baerends who suggest a new long-range-corrected xc kernel that shifts the orbital energy of the acceptor orbital to a value related to the electron affinity. The wrong asymptotic behavior of the CT states is corrected by a distance-dependent Coulomb term that corrects for electron transfer self-interaction.<sup>[181]</sup>

In recent years, TDDFT has been applied successfully, for example, to the investigation of energy- and electron-transfer processes between carotenoids and chlorophylls,<sup>[63,182,183]</sup> which has led to the correct prediction of a carotenoid radical cation during nonphotochemical quenching (NPQ). NPQ is a photosynthetic process by which plants protect themselves against photodamage under high light conditions.<sup>[184]</sup> Among other possible scenarios, one hypothesis for a molecular mechanism of NPQ is the formation of a quenching complex consisting of chlorophyll a (Chl) and the carotenoid zeaxanthin (Zea), the putative quencher.<sup>[183,185–187]</sup> Calculations of the excited states of a Chl-Zea complex along an intermolecular distance coordinate were performed to study the influence of complex formation on the excited states of the pigments, where a hybrid approach combining CIS calculations for the CT excited states and TDDFT calculations for the valence excited states had to be used to correctly describe the CT excited states, the valence excited states, and their relative energies in the complex.<sup>[63,182]</sup> These calculations have shown that in such complexes excess energy quenching is possible via two mechanisms. 1) At all distances the excitation energy can be transferred from Chl to Zea, since the  $S_1$  energy of Zea is lower than the  $Q_y$  energy of Chl (Figure 6). Having arrived in the  $S_1$  state of Zea, the excess energy is dissipated as heat. 2) At short distances below 5.5 Å, when a complex is formed, the chlorophyll excited state can also be quenched via electron transfer from Zea to Chl, which results in a carotenoid radical cation and a chlorophyll radical anion (Figure 6). Based on these calculations a femtosecond pump–probe experiment has been suggested, in which the  $Q_y$  state of Chl should be excited and the typical carotenoid radical cation signal around 1000 nm should be probed.<sup>[182]</sup> In the meantime, this experiment has been performed and the radical cation signal was observed only during NPQ, which is a strong hint for the existence of a Chl-Zea complex under NPQ conditions.<sup>[188]</sup>

Recently, carotenoid radical formation has also been observed in the light-harvesting complex 2 (LH2) of the purple bacterium *Rhodobacter sphaeroides* upon photoexcitation of the  $S_2$  state of the carotenoid spheroidene (Spher).<sup>[189]</sup> Although TDDFT yields spurious low-lying Spher-to-BChl CT excited states, calculations employing the above-mentioned hybrid approach between CIS and TDDFT<sup>[164]</sup> on Spher-BChl model complexes allowed the unambiguous identification of one energetically accessible Spher-to-BChl state explaining the previ-

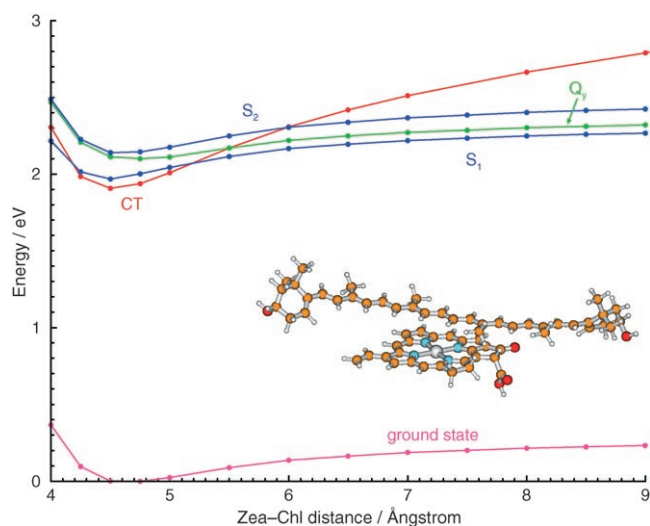


**Figure 6.** Potential energy curves of a putative chlorophyll a-zeaxanthin complex along an intermolecular separation coordinate calculated with a hybrid approach of TDDFT/BLYP/3-21G and CIS/3-21G. The structure of the model is given in the inset.

ous observation of the radical cation.<sup>[167,190]</sup> Analysis of the molecular orbitals of this state clearly shows that one electron is transferred from the highest molecular orbital located on Spher to the lowest unoccupied orbital located on BChl, undoubtedly revealing the CT nature of this state (Figure 7).

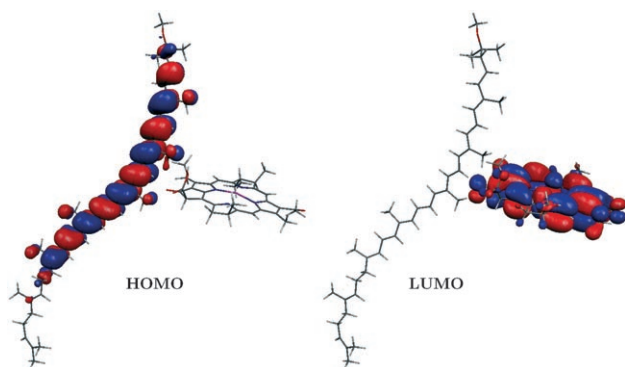


**Figure 7.** Highest occupied molecular orbital (HOMO, left) and lowest unoccupied molecular orbital (LUMO, right) of a spheroidene-bacteriochlorophyll model complex.

## 5. Analysis of Electronic Transitions

To gain physical insight into photoinitiated processes in biological systems, the electronic structure of the relevant excited states must be known. In principle, it is possible to analyze the full excited-state wavefunction or its electron density, and for this objective, the techniques developed for the analysis of the electronic ground state are simply applied to the excited state of interest. However, it is often easier and more elegant to address differences between the ground and excited state directly, thus avoiding tedious analysis of the complete excited-state wavefunction.

Usually, the electronic ground state of a molecular system is well represented by a single Slater determinant composed of single-electron wavefunctions describing the movement of the individual electrons in the molecule [Eq. (1)]. These single-electron wavefunctions correspond to the familiar molecular orbitals (MOs), which are well known to chemists and often used to understand molecular processes. It is thus natural to try to analyze the excited states, that is, their Slater determinants, with the help of the MOs. Sometimes indeed only one or two excited determinants contribute significantly to the excited-state wavefunction of interest, and in such cases its analysis is straightforward in terms of the occupied and virtual MOs that have been interchanged in the excited-state determinants compared to the ground state. Such a case is, for instance, the lowest charge-transfer excited state of the bacteriochlorophyll-spheroidene model complex (Figure 7), whose wavefunction is composed of essentially one Slater determinant in which the highest occupied MO (HOMO) of the ground state is replaced by the lowest unoccupied MO (LUMO). Hence, this excited state corresponds to a single-electron transition from the HOMO to the LUMO. Although the analysis of an electronic transition via MOs is computationally easy and thus convenient and straightforward for states with only one or two significantly contributing Slater determinants, it can become very tedious for states that are represented by several determinants with expansion coefficients of similar size.

Another possibility to obtain information about an electronic transition is to analyze the one-electron transition density. The transition density  $T(r)$  couples the electronic ground state with the excited state of interest and is in general given as Equation (29):

$$T(r) = N \int |\Psi_{\text{ex}}(r_1, r_2, \dots, r_n) \langle \Psi_0(r_1, r_2, \dots, r_n) | dr_1 \dots dr_n \quad (29)$$

In principle, one can analyze the transition density directly to obtain valuable information about the symmetry of the transition and about the way in which a one-electron operator couples two different states. It is, however, useful to analyze the transition density matrix, which is given in the molecular orbital basis as Equation (30):

$$(T)_{ia} = \langle \phi_i | \hat{T}(r) | \phi_a \rangle \quad (30)$$

via so-called “natural transition orbitals” analogous to the well-known natural orbitals obtained by diagonalization of the ground-state single-electron density.<sup>[191]</sup> Since the transition density matrix is a rectangular  $n_{\text{occ}} \times n_{\text{virt}}$  matrix, it cannot simply be diagonalized. Instead, the “corresponding orbital transformation” by Amos and Hall<sup>[192]</sup> can be applied, which is based on a singular value decomposition of the transition density matrix that yields pairs of occupied and virtual “natural transition orbitals”. Usually, an electronic transition can be expressed by one single occupied–virtual pair of the “natural transition orbitals”, even if the transition is highly mixed in the canonical molecular orbital basis, where it is thus difficult to analyze. Plotting the corresponding natural transition orbitals

gives detailed insight into the nature of the electronic transition. An example of the application of this analysis technique is given in ref. [191].

A complementary approach to the analysis of the transition density matrix  $\mathbf{T}$  is the investigation of the difference density matrix  $\Delta$ , which is simply given as the difference between the single-electron density matrices of the excited state  $\mathbf{P}_{\text{ex}}$  and that of the electronic ground state  $\mathbf{P}_0$  [Eq. (31)]:

$$\Delta = \mathbf{P}_{\text{ex}} - \mathbf{P}_0 \quad (31)$$

Today, the analysis of an electronic transition by means of the difference density is frequently performed (see, for example, refs. [193–196]) and, in principle, valence and Rydberg excited states can be easily distinguished. Also, the nature of the transition ( $n\pi^*$  or charge transfer) is often readily apparent for simple molecular systems. However, the difference density is a complicated function with often intricate nodal surfaces, which makes its plotting and analysis very tedious, especially for larger molecules. This is mostly due to the fact that both the ground-state electron density that is removed upon excitation and the “new” electron density of the excited state are shown with different signs together in one picture. It is also somewhat awkward that a density acquires a negative sign, since it is originally defined as the square of the wavefunction.

The physically most appealing and conceptually easiest way to analyze the nature of a complicated electronic transition is via so-called attachment/detachment density plots.<sup>[197,198]</sup> The basis of this analysis is the diagonalization of the difference density matrix  $\Delta$  given by Equation (31) via [Eq. (32)]:

$$\mathbf{U}^\dagger \Delta \mathbf{U} = \delta \quad (32)$$

where  $\mathbf{U}$  is a unitary transformation matrix containing the eigenvectors of the difference density matrix, which again could be considered as “natural orbitals of the electronic transition”, but which are generally different from those obtained from the diagonalization of the transition density matrix [Eq. (30)].  $\delta$  is a diagonal matrix containing the eigenvalues  $\delta_p$  of  $\Delta$ , which are interpreted as occupation numbers of the eigenvectors. The diagonal difference density matrix  $\delta$  is split into two matrices  $\mathbf{A}$  and  $\mathbf{D}$ . The matrix  $\mathbf{D}$ , the so-called detachment density, is defined as the sum of all eigenvectors of  $\Delta$  which possess negative eigenvalues, while the attachment density matrix  $\mathbf{A}$  is defined as the sum of all natural orbitals of the difference density matrix with positive occupation numbers, weighted by the absolute value of their occupation. This density matrix  $\mathbf{A}$  corresponds to the particle levels occupied in the electronic transition. The difference between the two new matrices  $\mathbf{A}$  and  $\mathbf{D}$  corresponds to the original difference density matrix  $\Delta$  [Eq. (33)]:

$$\Delta = \mathbf{A} - \mathbf{D} \quad (33)$$

In other words, the detachment density is that part of the single-electron ground-state density that is removed and rearranged as attachment density. Together these densities charac-

terize an electronic transition as  $\mathbf{D} \rightarrow \mathbf{A}$ , which permits the visualization and analysis of electronic transitions more or less as if they correspond to just single-orbital replacements, regardless of the extent of configuration mixing that occurs in the excited-state wavefunction and regardless of how inappropriate the molecular orbitals are for the description of the transition. The analysis via attachment/detachment density plots can be applied to any excited-state calculation that yields a one-particle difference density. As an example, the detachment/attachment density plot of the  $Q_y$  state of bacteriochlorophyll is shown in Figure 8, which has been calculated at the theoretical level of TDDFT/TDA/BLYP/6-31G\*. At this level of theory, this state corresponds to a linear combination of three contributing Slater determinants, and an analysis at the molecular orbital level would thus be tedious. The detachment/attachment density plots are much simpler and straightforward to interpret.

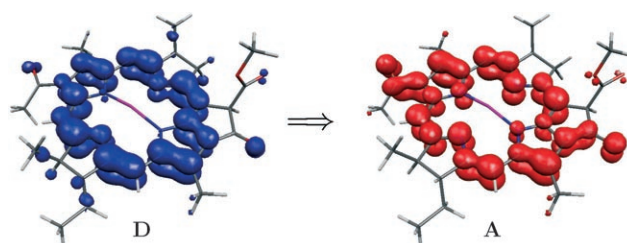


**Figure 8.** Detachment density  $\mathbf{D}$  and attachment density  $\mathbf{A}$ , which characterize the  $Q_y$  state of bacteriochlorophyll as a  $\pi\pi^*$  excited state.

## 6. Comparison and Perspectives of Theoretical Methods

In the previous sections, the most widely used theoretical methods to calculate electronically excited states of large molecules have been briefly reviewed. Their theoretical concepts and basic equations have been introduced and the properties and limitations of the methods have been pointed out. Successful applications of these methods to various photoinitiated processes in biological systems have been described.

We have seen that the cheapest wavefunction-based methods that are regularly applied to studying photoinitiated processes in biological systems are CIS and CASSCF. While the first is cheap but far too inaccurate to allow more than a rough and qualitative understanding of the relevant excited states, CASSCF can be very accurate if large enough basis sets and active spaces are employed, but this is computationally expensive and furthermore requires a significant amount of a priori knowledge and technical input. Semiempirical approaches such as INDO/S or OM2/MRCI offer an alternative to the cumbersome ab initio calculation of excited states, but their errors are essentially not predictable. However, there is hope that OM2/MRCI is a substantial improvement over previous semiempirical approaches, but further evaluation is needed. TDDFT and its variants represent at present the most widely used approaches for the investigation of photoinitiated processes in

biological systems. However, present-day TDDFT exhibits substantial errors for several classes of states that can be relevant for large molecules due to the employed exchange-correlation functionals. As a consequence, TDDFT calculations for large molecules or molecular aggregates must be performed with great care and with subsequent tedious analysis of the excited-state wavefunctions obtained.

A general problem of the calculation of excited states of large molecules is that even in the low-energy region, the relevant states can exhibit very different electronic structures. As an unfortunate consequence, any significant approximation introduced during the computation might be a reasonable approximation for one class of states but at the same time a very poor one for another equally important class of excited states. It is one thing to reproduce the spectrum of a molecule where only optically allowed states are relevant, which are mostly  $\pi\pi^*$  states and which thus belong to one class of states. It is much more challenging to also take account of dark states not visible in the spectrum, which very often have unusual electronic structures, for example, charge-transfer,  $n\pi^*$ ,  $n\sigma^*$ , and so on, but which can determine the dynamics of a photoinitiated process. This is, for instance, the case for TDDFT, which typically yields excellent results for  $\pi\pi^*$  excited states and thus reproduces electronic spectra quite favorably, but TDDFT fails completely to describe charge-transfer excited states, which for large molecular systems can occur at low energy and can be important for photoprocesses. The same argument holds for semiempirical models, since a chosen set of parameters for the one- and two-electron integrals will be appropriate for the description of some states, but probably be not suitable for others with a significantly different electronic structure. Even CASSCF with small active spaces encounters this problem, since a limited selection of active orbitals inevitably leads to an unbalanced treatment of excited states with very different electronic structures.

Another very general problem in the theoretical description of large molecular systems, and in particular in weakly interacting molecular complexes like the pigments in photosynthetic proteins, is the influence of van der Waals interactions and polarization. In general, these interactions determine the geometrical structure of the complexes, and need to be considered in QM/MM approaches aiming at the description of excited-state or ground-state dynamics. Consequently, correlated methods at the MP2 level or beyond should be used. However, at fixed geometries their influence on vertical excited states is only small, since errors in the description of these interactions basically cancel when excitation energies are calculated.

In summary, at present there exists no theoretical method for excited states of large molecules that fulfills all the requirements listed in the Introduction. Because of the arguments discussed above, it seems difficult and challenging to develop a cheap theoretical method that allows the reliable calculation of all excited states of large molecules with reasonable accuracy, which would be a necessary prerequisite for a successful QM/MM scheme for excited-state dynamics.

## Acknowledgements

The author gratefully acknowledges permanent support by Dr. Christine Hettmann-Dreuw. A.D. is funded by the Deutsche Forschungsgemeinschaft as an "Emmy-Noether" fellow.

**Keywords:** bioorganic chemistry · density functional calculations · excited states · photochemistry · quantum chemistry

- [1] D.-P. Häder, *Photosynthese*, Thieme, Stuttgart, 1999.
- [2] *Photosynthesis: From Light to Biosphere* (Ed.: P. Mathis), Kluwer, Dordrecht, 1996.
- [3] J. Wess, *Structure-Function Analysis of G Protein-Coupled Receptors*, Wiley-Liss, New York, 1999.
- [4] *Handbook of Photosensory Receptors* (Eds.: W. R. Briggs, J. L. Spudich), Wiley-VCH, Weinheim, 2005.
- [5] T. Ritz, S. Adem, K. Schulten, *Biophys. J.* **2000**, *78*, 707.
- [6] J. Gao, *Rev. Comput. Chem.* **1992**, *7*, 119.
- [7] A. R. Leach, *Molecular Modelling: Principles and Applications*, Longman, Essex, 1996.
- [8] R. G. Parr, W. Yang, *Density-Functional Theory of Atoms and Molecules*, Oxford Science Publication, New York, 1989.
- [9] R. M. Dreizler, E. K. U. Gross, *Density Functional Theory*, Springer, Heidelberg, 1995.
- [10] E. J. Baerends, O. V. Gritsenko, *J. Phys. Chem. A* **1997**, *101*, 5383.
- [11] S. Grimme, *Rev. Comput. Chem.* **2004**, *20*, 153.
- [12] T. Polivka, V. Sundström, *Chem. Rev.* **2004**, *104*, 2021.
- [13] J. del Bene, R. Ditchfield, J. A. Pople, *J. Chem. Phys.* **1971**, *55*, 2236.
- [14] J. B. Foresman, M. Head-Gordon, J. A. Pople, M. J. Frisch, *J. Phys. Chem.* **1992**, *96*, 135.
- [15] D. Hegarthy, M. A. Robb, *Mol. Phys.* **1979**, *38*, 1795.
- [16] R. H. E. Eade, M. A. Robb, *Chem. Phys. Lett.* **1981**, *83*, 362.
- [17] I. Frank, J. Hutter, D. Marx, M. Parinello, *J. Chem. Phys.* **1998**, *108*, 4060.
- [18] E. Runge, E. K. U. Gross, *Phys. Rev. Lett.* **1984**, *52*, 997.
- [19] M. E. Casida in *Recent Advances in Density Functional Methods, Part I* (Ed.: D. P. Chong), World Scientific, Singapore, 1995, p. 155.
- [20] A. Dreuw, M. Head-Gordon, *Chem. Rev.* **2005**, *105*, 4009.
- [21] J. E. Ridley, M. C. Zerner, *Theor. Chim. Acta* **1973**, *32*, 111.
- [22] M. Kotzian, N. Rösch, M. C. Zerner, *Theor. Chim. Acta* **1992**, *81*, 201.
- [23] W. Weber, W. Thiel, *Theor. Chem. Acc.* **2000**, *103*, 495.
- [24] P. Strodel, P. Tavan, *J. Chem. Phys.* **2002**, *117*, 4667.
- [25] P. Strodel, P. Tavan, *J. Chem. Phys.* **2002**, *117*, 4677.
- [26] R. J. Buenker, S. D. Peyerimhoff, W. Butscher, *Mol. Phys.* **1978**, *35*, 771.
- [27] R. J. Buenker, S. D. Peyerimhoff, P. J. Bruna in *Computational Theoretical Organic Chemistry* (Eds.: I. G. Csizmadia, R. Daudel), Reidel, Dordrecht, 1981, p. 91.
- [28] J. J. W. McDoull, K. Peasley, M. A. Robb, *Chem. Phys. Lett.* **1988**, *148*, 183.
- [29] B. O. Roos, K. Andersson, M. P. Fülscher, *Chem. Phys. Lett.* **1992**, *192*, 5.
- [30] K. Andersson, P.-Å. Malmqvist, B. O. Roos, *J. Chem. Phys.* **1992**, *96*, 1218.
- [31] B. O. Roos, K. Andersson in *Modern Electronic Structure Theory* (Ed.: D. R. Yarkony), World Scientific, Singapore, 1995, p. 55.
- [32] P. Celani, H.-J. Werner, *J. Chem. Phys.* **2000**, *112*, 5546.
- [33] S. Grimme, M. Waletzke, *Phys. Chem. Chem. Phys.* **2000**, *2*, 2075.
- [34] W. D. Laidig, R. J. Bartlett, *Chem. Phys. Lett.* **1984**, *104*, 424.
- [35] U. S. Mahapatra, B. Datta, B. Bandyopaghyay, D. Mukherjee, *Adv. Quantum Chem.* **1998**, *30*, 163.
- [36] K. Emrich, *Nucl. Phys. A* **1981**, *351*, 379.
- [37] H. Sekino, R. J. Bartlett, *Int. J. Quantum Chem. Symp.* **1984**, *18*, 255.
- [38] J. Geertsen, M. Rittby, R. J. Bartlett, *Chem. Phys. Lett.* **1989**, *164*, 57.
- [39] H. J. Monkhorst, *Int. J. Quantum Chem. Symp.* **1977**, *11*, 421.
- [40] E. Dalgaard, H. J. Monkhorst, *Phys. Rev. A* **1983**, *28*, 1217.
- [41] H. Koch, O. Christiansen, P. Jørgensen, *Chem. Phys. Lett.* **1995**, *244*, 75.
- [42] O. Christiansen, J. Gauss, B. Schimmelpennig, *Phys. Chem. Chem. Phys.* **2000**, *2*, 965.
- [43] H. Nakatsuji, K. Hirao, *J. Chem. Phys.* **1978**, *68*, 2053.

- [44] O. Christiansen, H. Koch, P. Jørgensen, *Chem. Phys. Lett.* **1995**, *243*, 409.
- [45] C. Haettig, F. Weigend, *J. Chem. Phys.* **2000**, *113*, 5154.
- [46] O. Christiansen, H. Koch, P. Jørgensen, *J. Chem. Phys.* **1995**, *103*, 7429.
- [47] H. Koch, O. Christiansen, P. Jørgensen, T. Helgaker, A. S. de Meras, *J. Chem. Phys.* **1997**, *106*, 1808.
- [48] M. Head-Gordon, R. J. Rico, M. Oumi, T. J. Lee, *Chem. Phys. Lett.* **1994**, *219*, 21.
- [49] M. Head-Gordon, D. Maurice, M. Oumi, *Chem. Phys. Lett.* **1995**, *246*, 114.
- [50] M. Oumi, D. Maurice, T. J. Lee, M. Head-Gordon, *Chem. Phys. Lett.* **1997**, *279*, 151.
- [51] E. V. Gromov, A. B. Trofimov, N. M. Vitkovskaja, J. Schirmer, H. Köppel, *J. Chem. Phys.* **2003**, *119*, 737.
- [52] A. B. Trofimov, G. Stelter, J. Schirmer, *J. Chem. Phys.* **2002**, *117*, 6402.
- [53] J. Schirmer, *Phys. Rev. A* **1982**, *26*, 2395.
- [54] J. Schirmer, A. B. Trofimov, *J. Chem. Phys.* **2004**, *120*, 11449.
- [55] B. O. Roos, *Adv. Chem. Phys.* **1987**, *69*, 399.
- [56] A. Szabo, N. S. Ostlund, *Modern Quantum Chemistry*, MacMillan, New York, **1982**.
- [57] R. McWeeny, B. T. Sutcliffe, *Methods of Molecular Quantum Mechanics*, Academic Press, London, **1969**.
- [58] C. D. Sherrill, H. F. Schaefer III, *Adv. Quantum Chem.* **1999**, *34*, 143.
- [59] D. Maurice, M. Head-Gordon, *Mol. Phys.* **1999**, *96*, 1533.
- [60] E. R. Davidson, *J. Comput. Phys.* **1975**, *17*, 87.
- [61] S. Hirata, M. Head-Gordon, R. J. Bartlett, *J. Chem. Phys.* **1999**, *111*, 10774.
- [62] J. F. Stanton, J. Gauss, N. Ishikawa, M. Head-Gordon, *J. Chem. Phys.* **1995**, *103*, 4160.
- [63] A. Dreuw, G. R. Fleming, M. Head-Gordon, *Phys. Chem. Chem. Phys.* **2003**, *5*, 3247.
- [64] C.-P. Hsu, P. J. Walla, M. Head-Gordon, G. R. Fleming, *J. Phys. Chem. B* **2001**, *105*, 11016.
- [65] I. N. Ragazos, M. A. Robb, F. Bernardi, M. Olivucci, *Chem. Phys. Lett.* **1992**, *197*, 217.
- [66] M. J. Bearpark, M. A. Robb, H. B. Schlegel, *Chem. Phys. Lett.* **1994**, *223*, 269.
- [67] F. Bernardi, M. Olivucci, M. A. Robb, *Chem. Soc. Rev.* **1996**, *25*, 321.
- [68] R. E. Stenkamp, S. Filipek, C. A. G. G. Driessen, K. Teller, D. C. Palczewski, *Biochim. Biophys. Acta* **2002**, *1565*, 168.
- [69] M. Garavelli, P. Celani, F. Bernardi, M. A. Robb, M. Olivucci, *J. Am. Chem. Soc.* **1997**, *119*, 6891.
- [70] A. Migani, M. A. Robb, M. Olivucci, *J. Am. Chem. Soc.* **2003**, *125*, 2804.
- [71] F. Blomgren, S. Larsson, *Chem. Phys. Lett.* **2003**, *376*, 704.
- [72] H. Köppel, W. Domcke, L. S. Cederbaum, *Adv. Chem. Phys.* **1984**, *57*, 59.
- [73] *Conical Intersections* (Eds.: W. Domcke, D. R. Yarkony, H. Köppel), World Scientific, Singapore, **2004**.
- [74] A. Sinicropi, A. Migani, L. De Vico, M. Olivucci, *Photochem. Photobiol. Sci.* **2003**, *2*, 1250.
- [75] L. De Vico, M. Garavelli, F. Bernardi, M. Olivucci, *J. Am. Chem. Soc.* **2005**, *127*, 2433.
- [76] O. Weingart, V. Buss, M. A. Robb, *Phase Transitions* **2005**, *78*, 17.
- [77] A. Migani, A. Sinicropi, N. Ferre, A. Cembran, M. Garavelli, M. Olivucci, *Faraday Discuss.* **2004**, *127*, 179.
- [78] A. Cembran, F. Bernardi, M. Olivucci, M. Garavelli, *J. Am. Chem. Soc.* **2004**, *126*, 16018.
- [79] J. Hufen, M. Sugihara, V. Buss, *J. Phys. Chem. B* **2004**, *108*, 20419.
- [80] N. Ferre, A. Cembran, M. Garavelli, M. Olivucci, *Theor. Chem. Acc.* **2004**, *112*, 335.
- [81] M. Schreiber, V. Buss, *Int. J. Quantum Chem.* **2003**, *95*, 882.
- [82] A. Cembran, F. Bernardi, M. Olivucci, M. Garavelli, *Proc. Natl. Acad. Sci. USA* **2005**, *102*, 6255.
- [83] A. Cembran, R. Gonzalez-Luque, P. Altoe, M. Merchan, F. Bernardi, M. Olivucci, M. Garavelli, *J. Phys. Chem. A* **2005**, *109*, 6597.
- [84] T. Andruniow, N. Ferre, M. Olivucci, *Proc. Natl. Acad. Sci. USA* **2004**, *101*, 17908.
- [85] P. B. Coto, A. Sinicropi, L. De Vico, N. Ferre, M. Olivucci, *Mol. Phys.* **2006**, *104*, 983.
- [86] I. Conti, F. Bernardi, G. Orlandi, M. Garavelli, *Mol. Phys.* **2006**, *104*, 915.
- [87] M. E. Martin, F. Negri, M. Olivucci, *J. Am. Chem. Soc.* **2004**, *126*, 5452.
- [88] P. Altoe, F. Bernardi, M. Garavelli, G. Orlandi, F. Negri, *J. Am. Chem. Soc.* **2005**, *127*, 3952.
- [89] A. Sinicropi, T. Andruniow, N. Ferre, R. Basosi, M. Olivucci, *Photochem. Photobiol. Sci.* **2003**, *2*, 1250.
- [90] K. J. Hellingwerf, J. Hendriks, T. Gensch, *J. Phys. Chem. A* **2003**, *107*, 1082.
- [91] G. Groenhof, M. Bouxin-Cademartory, B. Hess, S. P. de Visser, H. J. C. Berendsen, M. Olivucci, A. E. Mark, M. A. Robb, *J. Am. Chem. Soc.* **2004**, *126*, 4228.
- [92] Y. Yamada, S. Yamamoto, T. Yamato, T. Kakitani, *J. Mol. Struct.* **2001**, *536*, 195.
- [93] C. Ko, B. Levine, A. Toniolo, L. Manohar, S. Olsen, H.-J. Werner, T. J. Martinez, *J. Am. Chem. Soc.* **2003**, *125*, 12710.
- [94] A. Yamada, T. Ishikura, T. Yamato, *Proteins Struct. Funct. Bioinf.* **2004**, *55*, 1063.
- [95] A. L. Sobolewski, W. Domcke, *Eur. Phys. J. D* **2002**, *20*, 369.
- [96] A. L. Sobolewski, W. Domcke, C. Dedonder-Lardeux, C. Jouvet, *Phys. Chem. Chem. Phys.* **2002**, *4*, 1093.
- [97] A. L. Sobolewski, W. Domcke, *Phys. Chem. Chem. Phys.* **2004**, *6*, 2763.
- [98] S. Perun, A. L. Sobolewski, W. Domcke, *J. Am. Chem. Soc.* **2005**, *127*, 6257.
- [99] T. Schultz, E. Samoylova, W. Radloff, I. V. Hertel, A. L. Sobolewski, W. Domcke, *Science* **2004**, *306*, 1765.
- [100] S. Grimme, M. Waletzke, *J. Chem. Phys.* **1999**, *111*, 5645.
- [101] K. Tomić, J. Tatchen, C. M. Marian, *J. Phys. Chem. A* **2005**, *109*, 8410.
- [102] K. A. Seefeld, C. Plützer, D. Löwenich, T. R. L. Häber, K. Kleinermanns, J. Tatchen, C. M. Marian, *Phys. Chem. Chem. Phys.* **2005**, *7*, 3021.
- [103] C. M. Marian, D. Nolting, R. Weinkauff, *Phys. Chem. Chem. Phys.* **2005**, *7*, 3306.
- [104] J. A. Pople, G. A. Segal, *J. Chem. Phys.* **1965**, *43*, S136.
- [105] J. A. Pople, D. P. Santry, G. A. Segal, *J. Chem. Phys.* **1965**, *43*, S129.
- [106] R. Pariser, R. G. Parr, *J. Chem. Phys.* **1953**, *21*, 466.
- [107] N. Mataga, K. Nishimoto, *Z. Phys. Chem.* **1957**, *13*, 140.
- [108] J. A. Pople, D. L. Beveridge, P. A. Dobosh, *J. Chem. Phys.* **1967**, *47*, 2026.
- [109] G. McDermott, S. M. Prince, A. Freer, A. M. Hawthorne-White-Lawless, M. Z. Papiz, R. J. Cogdell, N. W. Isaacs, *Nature* **1995**, *374*, 517.
- [110] J. Köpke, X. Hu, C. Münke, K. Schulten, H. Michel, *Structure* **1996**, *4*, 581.
- [111] X. Hu, T. Ritz, A. Damjanovic, K. Schulten, *J. Phys. Chem. B* **1997**, *101*, 3854.
- [112] M. G. Cory, M. C. Zerner, X. C. Xu, K. Schulten, *J. Phys. Chem. B* **1998**, *102*, 7640.
- [113] M. F. Ng, Y. Zhao, G. H. Chen, *J. Phys. Chem. B* **2003**, *107*, 9589.
- [114] Y. Zhao, M. F. Ng, G. H. Chen, *Phys. Rev. E* **2004**, *69*, 032902.
- [115] A. Damjanovic, H. M. Vaswani, P. Fromme, G. R. Fleming, *J. Phys. Chem. B* **2002**, *106*, 10251.
- [116] X. J. Jordanides, G. D. Scholes, W. A. Shapley, J. R. Reimers, G. R. Fleming, *J. Phys. Chem. B* **2004**, *108*, 1753.
- [117] D. B. Cook, P. C. Hollis, R. M. Weeny, *Mol. Phys.* **1967**, *13*, 553.
- [118] F. Weinhold, J. E. Carpenter, *J. Mol. Struct.* **1988**, *165*, 189.
- [119] W. Koch, *Z. Naturforsch. A* **1993**, *48*, 819.
- [120] M. Wanko, M. Hoffmann, P. Strodel, A. Koslowski, W. Thiel, F. Neese, T. Frauenheim, M. Elstner, *J. Phys. Chem. B* **2005**, *109*, 3606.
- [121] P. Hohenberg, W. Kohn, *Phys. Rev.* **1964**, *136*, B864.
- [122] W. Kohn, L. J. Sham, *Phys. Rev.* **1965**, *140*, A1133.
- [123] H. Eschrig, *The Fundamentals of Density Functional Theory*, Teubner, Stuttgart, **1996**.
- [124] W. Koch, M. C. Holthausen, *A Chemist's Guide to Density Functional Theory*, Wiley-VCH, Weinheim, **2000**.
- [125] T. Ziegler, A. Rauk, E. J. Baerends, *Theor. Chim. Acta* **1977**, *43*, 261.
- [126] S. Grimme, C. Nonnenberg, I. Frank, *J. Chem. Phys.* **2003**, *119*, 11574.
- [127] S. Grimme, C. Nonnenberg, I. Frank, *J. Chem. Phys.* **2003**, *119*, 11585.
- [128] C. Nonnenberg, C. Bräuchle, I. Frank, *J. Chem. Phys.* **2005**, *122*, 014311.
- [129] C. C. J. Roothaan, *Rev. Mod. Phys.* **1960**, *32*, 179.
- [130] R. Car, M. Parinello, *Phys. Rev. Lett.* **1985**, *55*, 2471.
- [131] U. Röhrig, L. Guidoni, A. Laio, I. Frank, U. Röthlisberger, *J. Am. Chem. Soc.* **2004**, *126*, 15328.
- [132] R. van Leeuwen, *Phys. Rev. Lett.* **1999**, *82*, 3863.
- [133] R. van Leeuwen, *Int. J. Mod. Phys. B* **2001**, *15*, 1969.
- [134] E. K. U. Gross, W. Kohn, *Adv. Quantum Chem.* **1990**, *21*, 255.
- [135] K. Yabana, G. F. Bertsch, *Phys. Rev. B* **1996**, *54*, 4484.
- [136] M. A. L. Marquez, A. Castro, G. F. Bertsch, A. Rubio, *Comput. Phys. Commun.* **2003**, *151*, 60.

- [137] A. Castro, M. A. L. Marquez, J. A. Alonso, G. F. Bertsch, K. Yabana, A. Rubio, *J. Chem. Phys.* **2002**, *116*, 1930.
- [138] M. A. L. Marquez, X. Lopez, D. Varsano, A. Castro, A. Rubio, *Phys. Rev. Lett.* **2003**, *90*, 258101.
- [139] S. Hirata, M. Head-Gordon, *Chem. Phys. Lett.* **1999**, *314*, 291.
- [140] F. Furche, *J. Chem. Phys.* **2001**, *114*, 5982.
- [141] P. A. M. Dirac, *Proc. Cambridge Philos. Soc.* **1930**, *26*, 376.
- [142] S. H. Vosko, L. Wilk, M. Nusair, *Can. J. Phys.* **1980**, *58*, 1200.
- [143] A. D. Becke, *Phys. Rev. A* **1988**, *38*, 3098.
- [144] C. Lee, W. Yang, R. G. Parr, *Phys. Rev. B* **1988**, *37*, 785.
- [145] J. P. Perdew, K. Burke, M. Enzerhof, *Phys. Rev. Lett.* **1996**, *77*, 3865.
- [146] J. P. Perdew, K. Burke, M. Enzerhof, *Phys. Rev. Lett.* **1997**, *78*, 1396.
- [147] A. D. Becke, *J. Chem. Phys.* **1993**, *98*, 5648.
- [148] J. Frenkel, *Wave Mechanics, Advanced General Theory*, Clarendon, Oxford, **1934**.
- [149] J. Heinrichs, *Chem. Phys. Lett.* **1968**, *2*, 315.
- [150] P. Ring, P. Schuck, *The Nuclear Many-Body Problem*, Springer, Heidelberg, **1980**.
- [151] A. L. Fetter, J. D. Walecka, *Quantum Theory of Many-Particle Systems*, McGraw-Hill, New York, **1971**.
- [152] D. J. Thouless, *The Quantum Mechanics of Many-Body Systems*, Academic Press, New York, **1972**.
- [153] S. Grimme, *Chem. Phys. Lett.* **1996**, *259*, 128.
- [154] T. A. Niehaus, S. Suhai, F. Della Sala, P. Lugli, M. Elstner, G. Seifert, T. Fraunheim, *Phys. Rev. B* **2001**, *63*, 085108.
- [155] K. Eichkorn, O. Treutler, H. Öhm, M. R. A. Häser, *Chem. Phys. Lett.* **1995**, *240*, 283.
- [156] C. Jamorski, M. E. Casida, D. R. Salahub, *J. Chem. Phys.* **1996**, *104*, 5134.
- [157] R. Bauernschmitt, M. Häser, O. Treutler, R. Ahlrichs, *Chem. Phys. Lett.* **1997**, *264*, 573.
- [158] J. L. Weisman, M. Head-Gordon, *J. Am. Chem. Soc.* **2001**, *123*, 11686.
- [159] A. Dreuw, J. Plötner, L. Lorenz, J. Wachtveitl, J. E. Djanhan, J. Brüning, M. Bolte, M. U. Schmidt, *Angew. Chem.* **2005**, *117*, 7961; *Angew. Chem. Int. Ed.* **2005**, *44*, 7783.
- [160] R. J. Cave, F. Zhang, N. T. Maitra, K. Burke, *Chem. Phys. Lett.* **2004**, *389*, 39.
- [161] N. T. Maitra, F. Zhang, R. J. Cave, K. Burke, *J. Chem. Phys.* **2004**, *120*, 5932.
- [162] Z.-L. Cai, K. Sendt, J. R. Reimers, *J. Chem. Phys.* **2002**, *117*, 5543.
- [163] S. Grimme, M. Parac, *ChemPhysChem* **2003**, *3*, 292.
- [164] A. Dreuw, J. L. Weisman, M. Head-Gordon, *J. Chem. Phys.* **2003**, *119*, 2943.
- [165] D. J. Tozer, *J. Chem. Phys.* **2003**, *119*, 12697.
- [166] A. L. Sobolewski, W. Domcke, *Chem. Phys.* **2003**, *294*, 73.
- [167] A. Dreuw, M. Head-Gordon, *J. Am. Chem. Soc.* **2004**, *126*, 4007.
- [168] C. Van Caillie, R. D. Amos, *Chem. Phys. Lett.* **1999**, *308*, 249.
- [169] C. Van Caillie, R. D. Amos, *Chem. Phys. Lett.* **2000**, *317*, 159.
- [170] F. Furche, R. Ahlrichs, *J. Chem. Phys.* **2002**, *117*, 7433.
- [171] M. Dierksen, S. Grimme, *J. Chem. Phys.* **2004**, *120*, 3544.
- [172] M. Dierksen, S. Grimme, *J. Phys. Chem. A* **2004**, *108*, 10225.
- [173] L. Bernasconi, M. Sprik, J. Hutter, *J. Chem. Phys.* **2003**, *119*, 12417.
- [174] Y. Tawada, T. Tsuneda, S. Yanagisawa, T. Yanai, K. Hirao, *J. Chem. Phys.* **2004**, *1210*, 8425.
- [175] T. Yanai, D. P. Tew, N. C. Handy, *Chem. Phys. Lett.* **2004**, *393*, 51.
- [176] R. Baer, D. Neuhauser, *Phys. Rev. Lett.* **2005**, *94*, 043002.
- [177] H. Stoll, A. Savin in *Density Functional Methods in Physics* (Eds.: R. M. Dreizler, J. da Providencia), Plenum, New York, **1985**, p. 177.
- [178] A. Savin in *Recent Developments and Applications of Modern Density Functional Theory* (Ed.: J. M. Seminario), Elsevier, Amsterdam, **1996**.
- [179] T. Leininger, H. Stoll, H.-J. Werner, A. Savin, *Chem. Phys. Lett.* **1997**, *275*, 151.
- [180] H. Iikura, T. Tsuneda, T. Yanai, K. Hirao, *J. Chem. Phys.* **2001**, *115*, 5340.
- [181] O. Gritsenko, E. J. Baerends, *J. Chem. Phys.* **2004**, *121*, 655.
- [182] A. Dreuw, G. R. Fleming, M. Head-Gordon, *J. Phys. Chem. B* **2003**, *107*, 6500.
- [183] A. Dreuw, G. R. Fleming, M. Head-Gordon, *Biochem. Soc. Trans.* **2005**, *33*, 858.
- [184] A. M. Gilmore, *Physiol. Plant* **1997**, *99*, 197.
- [185] H. A. Frank, A. Cua, V. Chynwat, A. Young, A. Gosztola, M. R. Wasielewski, *Photosynth. Res.* **1994**, *41*, 389.
- [186] A. J. Young, H. A. Frank, *J. Photochem. Photobiol. B* **1996**, *36*, 3.
- [187] Y.-Z. Ma, N. E. Holt, X.-P. Li, K. K. Niyogi, G. R. Fleming, *Proc. Natl. Acad. Sci. USA* **2003**, *100*, 4377.
- [188] N. E. Holt, D. Zigmantas, L. Valkunas, X.-P. Xi, K. K. Niyogi, G. R. Fleming, *Science* **2005**, *307*, 433.
- [189] T. Polivka, D. Zigmantas, J. L. Herek, Z. He, T. Pascher, T. Pulleritis, R. J. Cogdell, H. A. Frank, V. Sundström, *J. Phys. Chem. B* **2002**, *106*, 11016.
- [190] M. Wormit, A. Dreuw, unpublished results.
- [191] R. L. Martin, *J. Chem. Phys.* **2003**, *118*, 4775.
- [192] A. T. Amos, G. G. Hall, *Proc. R. Soc. London Ser. A* **1961**, *263*, 483.
- [193] T. Climent, R. Gonzalez-Luque, M. Merchan, *J. Phys. Chem. A* **2003**, *107*, 6995.
- [194] L. Serrano-Andres, M. Merchan, M. Jablonski, *J. Chem. Phys.* **2003**, *119*, 4294.
- [195] V. Molina, M. Merchan, *J. Phys. Chem. A* **2001**, *105*, 3745.
- [196] K. B. Wiberg, C. M. Hadad, J. B. Foresman, W. A. Chupka, *J. Phys. Chem.* **1992**, *96*, 10756.
- [197] M. Head-Gordon, A. M. Grana, D. Maurice, C. A. White, *J. Phys. Chem.* **1995**, *99*, 14261.
- [198] A. M. Grana, T. J. Lee, M. Head-Gordon, *J. Phys. Chem.* **1995**, *99*, 3493.

Received: February 2, 2006

Revised: June 28, 2006

Published online on September 29, 2006